

## **PART II**



## **APPENDIX II.1**

# **EVALUATION OF REPTATION MODELS FOR PREDICTING THE LINEAR VISCOELASTIC PROPERTIES OF ENTANGLED LINEAR POLYMERS**

E. van Ruymbeke, R. Keunings,  
V. Stéphenne, A. Hagenaaars, C. Bailly

### **1.1 INTRODUCTION**

Understanding and predicting viscoelastic response of polymer melts from the knowledge of molecular structure has been an enduring issue in polymer science<sup>1,2,3,4</sup>. It has important ramifications for very practical as well as fundamental questions. Indeed, satisfactory physical models can be used to help predict processing performance as well as clarify molecular dynamics in the melt.

A very elegant approach to modeling of polymer melt viscoelasticity is based on scaling and reptation concepts pioneered by de Gennes<sup>1</sup> and developed by Edwards and Doi<sup>2</sup>. Those have long been restricted to qualitative predictions even in the case of linear viscoelasticity of

purely linear polymers (which is the focus of this paper) and seemed unable until recently to reach quantitative prediction levels. Two major reasons explained this limitation. First, pure reptation as described by de Gennes oversimplifies the true dynamics of linear chains in the melt. Besides curvilinear diffusion of a chain in the tube formed by entanglements with its neighbours (and itself), other relaxation mechanisms play an important role. Those mechanisms tend to accelerate stress relaxation. They include

- *tube length fluctuation* effects which speed up relaxation of segments close to chain ends while leaving internal segments unaffected<sup>2,3</sup>.
- *constraint release mechanisms* which can be modeled by *double reptation*<sup>5,6</sup> or *Rouse-type relaxation* of the tube<sup>7,8</sup>. In this paper we focus on double reptation which explicitly describes entanglements as binary events. An entanglement disappears (and hence a constraint is released) whenever a chain-end passes beyond the entanglement. This has two effects : orientational relaxation rates are increased in comparison with simple reptation and the frequency (or equivalent time) range of the relaxation is broadened<sup>6</sup>.

The second limitation comes from the intrinsically polydisperse nature of synthetic polymers. A mixing rule has to be found which weighs contributions from various chain lengths and their mutual interactions. Linear mixing rules utterly fail from a quantitative standpoint<sup>6,9,10</sup>. This results from the coupling between relaxation functions of chains having different lengths. The presence of short chains speeds up relaxation of longer ones and vice-versa. Double reptation accounts for these effects in a very natural manner and is frequently invoked<sup>6,10,11</sup> although other (complementary) approaches are also known<sup>4,8,12</sup>. Recently, generalized mixing rules derived from double reptation have been proposed<sup>9,13,14</sup>.

A flurry of recent studies has refined early reptation models by incorporating some or all of the above-mentioned refinements<sup>3,4,15</sup>. As a consequence, quantitative predictions of linear viscoelasticity from knowledge of molecular distribution are now available. However, the question of the best overall model for linear polydisperse polymers has not been answered unequivocally. In particular, one of the more

sophisticated reptation models, the so-called time dependent diffusion reptation by des Cloizeaux (TDD)<sup>16</sup>, has received little attention. To our knowledge, only two papers have used TDD with double reptation (TDD-DR) for quantitative predictions of linear viscoelastic functions from MWD, in addition to the two papers by des Cloizeaux himself<sup>16,17</sup>. The first paper is by Wasserman and Grassley<sup>11</sup>, who assumed a universal relation between the TDD parameters  $M^*$  and  $Me$  (i.e.  $M^* = 12.5 Me$ ), a relation which des Cloizeaux<sup>16</sup> obtained from fits of polybutadiene data only. This assumption is not a valid one, as shown by des Cloizeaux himself<sup>17</sup> using data for other materials (PMMA, PS, PI), and as confirmed in the present paper. The second paper is by Maier et al.<sup>9</sup>, who claimed that TDD gives worse results than those obtained with the simpler kernels (single exponential, Doi-Edwards). Thus, TDD has been scarcely tested following its introduction by des Cloizeaux. To our knowledge, it has never been compared to the tube-length fluctuations model by Doi and Edwards<sup>2</sup>.

As stated by des Cloizeaux<sup>17</sup>, "To test the theories, one needs very precise measurements made under similar conditions on sets of good monodisperse (or polydisperse) samples corresponding to different and well-defined molecular masses." The main objective of this paper is to provide such a systematic comparison. Linear viscoelasticity data have been obtained for polymers exhibiting contrasting ranges of dynamic behavior in the melt (polystyrene, polycarbonate and high density polyethylene). Some samples have been separated in narrow fractions to clarify their viscoelastic response. Extreme care has been taken in all cases to ensure confidence about the solution molecular characterization. Predictions from the models have been checked against the experimental data and conclusions drawn about the best overall model.

A second objective of this paper is to provide a sound basis for solving the so-called "inverse problem" i.e. predicting molecular structure from knowledge of viscoelastic response. The inverse problem is just as vitally important as the "direct problem" since it relates closely to molecular characterization and design of molecular structure for desired performance. The inverse problem is plagued by the so-called

“ill-posedness” issue, which is linked to its mathematical structure<sup>3,15</sup>. In a companion paper<sup>18</sup>, we will start from the conclusions of the present article to develop a methodology for solving the inverse problem, using the same set of experimental data. In particular, we will show that a descriptive continuity between reptation and Rouse motions is essential for quantitative inverse predictions when the polymer has a low degree of entanglement. In the present paper, a modified treatment for Rouse relaxation is included in order to provide the required continuity.

## 1.2 THEORY

### 1.2.1 Reptation models

According to Tsenoglou<sup>5,10</sup> and des Cloizeaux<sup>6</sup>, the relaxation modulus  $G(t)$  of a linear polymer melt is related to the molecular weight distribution  $w(M)$  through the mixing rule:

$$G(t) = G_N^0 \cdot \left( \int_{\log M_e}^{\infty} [F_{mono}(t, M)]^{\frac{1}{\beta}} \cdot w(M) d \log M \right)^{\beta}, \quad (1)$$

where  $G_N^0$  is the plateau modulus,  $w(M) = dW(M)/d \log(M)$  with  $W(M)$  the weight fraction of chains with molecular weight below  $M$ , and  $F_{mono}$  is the relaxation function of the monodisperse polymer of mass  $M$ . The exponent  $\beta$  was originally<sup>6,10</sup> set to a value of 2, according to the double reptation concept. Values of  $\beta$  slightly higher than 2 have been proposed, which could represent contributions of higher order entanglements, or could be linked to the tube dilation model<sup>8,12</sup>.

Validity of the mixing rule (1) can in principle be tested independently of reptation models once the relaxation function of monodisperse samples is obtained experimentally for a range of molecular weights. In practice, however, it is impossible to generate truly monodisperse

samples for such a test. It is certainly the case for industrial polymers such as HDPE and PC. More importantly, since our ultimate goal (addressed in the companion paper<sup>18</sup>) is the inverse problem, an analytical expression for the relaxation function is required. Therefore the predictive ability of various reptation models has to be tested. The starting point is the classical Doi and Edwards (DE) reptation theory<sup>2</sup>. The DE model computes the relaxation function from the curvilinear diffusion of a test chain through a virtual tube made of a fixed network of obstacles. In this basic simple reptation theory, relaxation of the surrounding chains forming the tube is assumed to have no influence on the test chain. The resulting relaxation function  $F_{DE}$  is given by equation 2 in Table 1. It involves two material parameters,  $K$  and  $\alpha$ , which link the reptation time  $\tau_{rept}$  to molecular weight. The basic reptation theory would imply that  $\alpha$  is exactly 3, but experimental values are closer to 3.4.

Table 1: Kernel functions and associated parameters

Models	Simple reptation relaxation function, $F_{sr}(t, M)$	Parameters
<b>Doi and Edwards</b>	$F_{DE}(t, M) = \frac{8}{\pi^2} \cdot \sum_{p \text{ odd}} \frac{1}{p^2} \cdot \exp\left(\frac{-p^2 \cdot t}{\tau_{rept}}\right)$ <p style="text-align: right;">(2)</p>	<b>K, <math>\alpha</math>:</b> $\tau_{rept} = K \cdot M^\alpha$

<b>Doi and Edwards with fluctuations</b>	$F_{\text{fluct}}(t, M) = \int_0^1 \exp\left(-\frac{t}{\tau_{\text{fluct}}}\right) d\xi \quad (3)$ $\tau_{\text{fluct}} = N \cdot \xi^4 \cdot \frac{\tau_{\text{rept}}(M)}{16 \cdot \nu^2} \quad \text{for } 0 < \xi < \xi_{\text{crit.}}$ $\tau_{\text{fluct}} = \left(\xi - \frac{\nu}{\sqrt{N}}\right)^2 \cdot \tau_{\text{rept}}(M) \quad \text{for } \xi_{\text{crit.}} < \xi < 1$	<b>K, <math>\nu</math>:</b> $\tau_{\text{rept}} = K \cdot M^3$ $\xi_{\text{crit.}} = \frac{2 \cdot \nu}{\sqrt{N}}$
<b>des Cloizeaux</b>	$F_{\text{TDD}}(t, M) = \frac{8}{\pi^2} \cdot \sum_{p \text{ odd}} \frac{1}{p^2} \cdot \exp(-p^2 \cdot U(t)) \quad (4)$ $U(t) = \frac{t}{\tau_{\text{rept}}} + \frac{1}{H} \cdot g\left(\frac{H \cdot t}{\tau_{\text{rept}}}\right)$ $g(y) = \sum_{n=1}^{\infty} \frac{1 - \exp(-n^2 \cdot y)}{n^2}$ $g(y) = -y + y^{0.5} \cdot \left[ y + (\pi \cdot y)^{0.5} + \pi \right]^{0.5}$ <p>(simplified form) <span style="float: right;">(5)</span></p>	<b>K, <math>M^*</math>:</b> $\tau_{\text{rept}} = K \cdot M^3$ $H = \frac{M}{M^*}$

The Doi and Edwards relaxation function can be improved by including fluctuations of the tube length around its equilibrium value<sup>2,3</sup>. Indeed, fast Rouse motions of chain segments in the vicinity of the tube ends allow the chain to explore some regions situated outside the original tube. These effects become important for a low degree of entanglement. Fluctuations depend only on molar mass and polymer nature. The resulting fluctuation relaxation function  $F_{\text{fluct}}$  is given by equation 3 in Table 1. Here,  $\nu$  is a material constant,  $N$  is the

number of entanglements per chain, and  $\tau_{rept}$  is the reptation time of the test chain. The latter is proportional to  $M^3$ , since fluctuations are already explicitly taken into account in the definition of  $\tau_{fluct}$ . Consequently,  $F_{fluct}$  only contains two material parameters:  $K$  and  $\nu$ .

A second development of the basic DE theory is the time-dependent diffusion model ( $F_{TDD}$ ) proposed by des Cloizeaux<sup>16</sup>. It also describes a chain relaxing in a fixed network of obstacles, but considers a time-dependent curvilinear diffusion coefficient  $D(t)$ . Immediately after a step strain,  $D(t)$  is singular because of fast Rouse motions which are not hampered by the tube. In this Rouse-dominated regime,  $D(t)$  is proportional to  $t^{-1/2}$ . At later times, reptation dominates and the diffusion coefficient becomes equal to its constant value predicted by the DE theory. These two extreme regimes and the transition in between are described by the relaxation function  $F_{TDD}$  given by equation 4 in Table 1. Here, the function  $U(t)$  consists of two terms. The first one represents relaxation by reptation and is identical to the corresponding term in  $F_{DE}$ . The second term specifically represents contributions of fluctuations. The weight of the fluctuation term depends on the value of a new material parameter  $M^*$ . The relationship between  $M^*$  and  $M_e$  (molecular weight between entanglements) is not completely understood. Some authors<sup>9,11</sup> initially proposed a universal relationship between the two, but this does not seem to hold (as confirmed by the results of des Cloizeaux<sup>17</sup> and the present work). The ratio  $M^*/M_e$  is found to be a decreasing function of  $M_e$ .  $K$  and  $M^*$  are the only two material parameters of the  $F_{TDD}$  relaxation function;  $\alpha$  is not a material parameter but has a fixed value of 3.

At this point, we have three candidate relaxation functions ( $F_{DE}$ ,  $F_{fluct}$ ,  $F_{TDD}$ ) to describe the behaviour of a monodisperse polymer. These have been derived assuming a fixed network of entanglements, thus neglecting constraint release processes. We collectively refer to them as  $F_{sr}$ , for simple reptation relaxation functions. Inclusion of double reptation is performed according to Tsenglou<sup>5,10</sup> and des Cloizeaux<sup>6</sup> in the following way:

$$F_{mono}(t, M) = F_{sr}(t, M)^{\beta}. \quad (5)$$

All ingredients of the mixing rule (1) are thus defined. There remains to discuss the way we consider the Rouse relaxation process.

### 1.2.2 Rouse relaxation

When macromolecules in the melt are not constrained by entanglements ( $M < Me$ ), their relaxation process results only from monomer friction and is described by the Rouse mechanism<sup>2,19,20</sup>. The time  $\tau_{Rouse}(M)$  is interpreted as the time needed by an unentangled chain to relax after a step strain. It is proportional to the square of the molar mass and in practice, the proportionality factor  $K_{Rouse}$  is specified by curve fitting. This relaxation process includes a large number of modes: after a time of  $\tau_{Rouse}/i^2$ , subchains with molar mass  $M/i$  have relaxed (see equation 7 in Table 2).

Table 2: Rouse relaxation in unentangled and entangled polymer melts

	<i>Rouse modulus</i>	<i>Parameters</i>
<b>Dilute solution and unentangled melt</b>	$G_{\text{Rouse}}(t) = \frac{\rho RT}{M} \cdot \sum_{p=1}^{\infty} \exp\left(\frac{-p^2 \cdot t}{\tau_{\text{Rouse}}(M)}\right)$ $= G_N^0 \cdot \sum_{p=1}^{\infty} \frac{1}{N} \cdot \exp\left(\frac{-p^2 \cdot t}{\tau_{\text{Rouse}}(M)}\right)$ <p style="text-align: right;">(7)</p>	<b><math>K_{\text{Rouse}}</math>:</b> $\tau_{\text{Rouse}} = K_{\text{Rouse}} \cdot M^2$ $N = M/M_e$
<b>Entangled polymer melt</b>	$G_{\text{Rouse}}(t) = G_N^0 \sum_{p=N}^{\infty} \frac{1}{N} \exp\left(\frac{-p^2 t}{\tau_{\text{Rouse}}(M)}\right)$ $+ \frac{1}{3} G_N^0 \sum_{p=1}^N \frac{1}{N} \exp\left(\frac{-p^2 t}{\tau_{\text{Rouse}}(M)}\right)$ <p style="text-align: right;">(8)</p>	<b><math>K_{\text{Rouse}}</math>:</b> $\tau_{\text{Rouse}} = K_{\text{Rouse}} \cdot M^2$ $N = M / M_e$

For entangled polymers, relaxation processes at times much shorter than the reptation time are also dominated by the Rouse mechanism<sup>2,19,20</sup>. There is however a significant difference with respect to dilute solutions or unentangled polymer melts. After a time equal to  $\tau_{\text{Rouse}}/N^2$ , where  $N$  represents the number of entanglements of the test chain, subchains with molar mass  $M_e$  are relaxed and the Rouse relaxation of longer subchains is hampered by the presence of the tube. Therefore, Rouse modes perpendicular to the tube cannot be activated for subchains longer than  $M_e$ . From this moment on the chain segments feel the constraint imposed by the tube, and only longitudinal Rouse modes along the tube remain to be considered. This leads to equation 8 in Table 2. The first term represents the

Rouse relaxation process of the whole chain restricted to subchains smaller than  $M_e$ , and the second term considers the slower modes, but only in the longitudinal dimension (hence the factor  $1/3$ ). The basis of this expression comes from a formula proposed by Pattamaprom et al.<sup>4</sup>. Nevertheless, it differs by a factor  $(1/N)$  in front of the exponentials. Indeed, Rouse relaxation of subchains shorter than the tube diameter must be identical to that of dilute polymer solutions or unentangled melts. This equivalence is guaranteed by the expression in Table 2 but not by the original formula by Pattamaprom et al.. The modified equation also reflects the well known divergence of the Rouse modulus at vanishing times.

Our treatment of the Rouse relaxation differs from those of Carrot et al.<sup>15</sup> or Leonardi et al.<sup>3</sup>. Both groups consider all Rouse modes of a subchain with a molar mass  $M_e$ . They do not take into account the fact that this subchain is, in reality, part of a longer chain. In addition, Leonardi et al.<sup>3</sup> consider an additional term which describes the slowest relaxation modes of the entire chain.

The Rouse contribution to the relaxation modulus,  $G_{\text{Rouse}}$ , is simply added to the reptation contribution expressed by equation 1.

## 1.3 EXPERIMENTS

### 1.3.1 Materials and samples preparation

Three kinds of linear polymers have been studied in this work: polystyrene (PS), polycarbonate (PC) and high density polyethylene (HDPE). This choice reflects our goal to cover a broad range molecular weight between entanglements.

Table 3: Molecular characterization of polystyrene samples

a) monodisperse

	Polydispersity	$M_w$ (g/mol)	$M_n$ (g/mol)
PS1	1.02	355500	346200
PS2	1.02	191300	187600
PS3	1.09	886900	813500
PS4	1.04	176700	169900
PS5	1.03	60400	58600
PS6	1.03	58400	56900

b) bidisperse

	Composition
PS7	50% PS2, 50% PS3
PS8	80% PS2, 20% PS6
PS9	20% PS4, 80% PS5

Table 4: Molecular characterization of polycarbonate samples

	Polydispersity	$M_w$ (g/mol)	$M_n$ (g/mol)	$M_z$ (g/mol)
PC1	2.35	22700	9600	34600
PC2	2.05	11300	5700	17400
PC3	1.51	23200	15300	30500
PC4	1.38	39000	28000	48500

Table 5: Molecular characterization of polyethylene samples

	Polydispersity	$M_w$ (g/mol)	$M_n$ (g/mol)	$M_z$ (g/mol)
PE1	4.9	145700	29700	677500
PE2	1.7	87000	51700	147000
PE3	1.9	121200	62600	338500
PE4	1.9	136000	70000	387000

Narrow dispersed anionically polymerized polystyrene samples have been kindly provided by Dr Deffieux from CNRS-ENSPCB (Bordeaux, France; samples PS3 and PS6 in Table 3a) and by Prof Friedrich from FMF (Freiburg, Germany; sample PS7) or purchased from Tosoh Co (TSK chromatographic standards PS1, PS2 and PS8). Bi or tri-disperse PS samples (PS9, PS12 and PS13 in Table 3b) are prepared by solution blending. For blending, components are first dissolved in THF at room temperature. After stirring for 1 h, the

solution is precipitated in methanol. The precipitate is then filtered and dried under vacuum until constant weight. Chemical stabilization of all samples is ensured by addition of Irganox 1076 (3000 ppm) antioxidant. For rheological experiments, the stabilized samples are dried (again) under vacuum at 110°C during 6 h. They are next compression-molded in the form of circular disks (thickness  $\cong$  1.5 mm, diameter  $\cong$  25 mm) on a Fontejne press at 175°C. The chromatographic and rheological data of PS10 and PS11 have been kindly supplied by Prof Friedrich from FMF (Freiburg, Germany) to provide an independent check and comparison with published data<sup>9</sup>.

PC1 (see Table 4) is a commercially available linear bisphenol-A polycarbonate made by interfacial phosgenation. It has been kindly supplied by GE Plastics (Bergen op Zoom, The Netherlands). PC2 to PC4 are preparative size fractions of PC1. They have been obtained by Continuous Polymer Fractionation (CPF)<sup>21</sup> according to the procedure reported in reference 22. For rheological experiments, PC powders are pre-dried at 120°C overnight and subsequently pressed to compact circular pellets (10 mm diameter, 2 mm thick) at room temperature using a hydraulic press. The pellets are then again dried under vacuum at 120°C overnight, prior to measurement.

PE1 is a broad industrial HDPE sample, prepared via multi-site Ziegler-Natta catalyst with density 0.958 and branching level below NMR spectroscopic detection limits. PE2, PE3 and PE4 are narrow-disperse fractions obtained by Successive Solution Fractionation (SSF) of PE1 in cyclohexanone according to the procedure described in reference 23. Resulting molecular weight distributions for the broad sample and the corresponding fractions are presented in Figure 1(a). In order to avoid degradation during rheological measurement, PE powders are stabilized with Irganox B215 (3000 ppm) and eventually compression-molded into circular disks in a Fontejne press at 175°C (thickness  $\cong$  1.5 mm, diameter  $\cong$  25 mm).

### 1.3.2 Size Exclusion Chromatography (SEC)

Solution characterization of the samples is reported in Tables 3 to 5.

**PC :** SEC-UV measurements are obtained on a system consisting of a Waters model 590 pump, a Waters WISP 717 device and a Waters 486 tuneable UV absorbance detector operating at 254 nm. Filtered PC samples in methylene chloride (0.1 w/v%) are injected in the system at an injection volume of 50 $\mu$ l. Two PL-gel 5 $\mu$  300x7.5 mm columns, (10<sup>3</sup> and 10<sup>5</sup> Å) are used in series with methylene chloride as mobile phase at a flow rate of 1.0 ml/min. Narrow PS standards (between 900000 and 1300 MW) and light scattering PC standards are used for calibration purposes. Absolute PC are obtained by universal calibration from the following Mark-Houwink relationships<sup>24</sup>:  $[\eta]_{PC} = 1.19 \cdot 10^{-4} * M^{0.80}$  (dl/g), and  $[\eta]_{PS} = 0.61 \cdot 10^{-4} * M^{0.74}$  (dl/g).

Results of universal calibration are checked against the available absolute PC standards and the agreement is within experimental error. Universal calibration is therefore preferred because a much broader MW range is covered by the PS standards than by the available PC standards. Resulting molecular weight distributions for the broad sample and the corresponding fractions are presented in Figure 1(a).

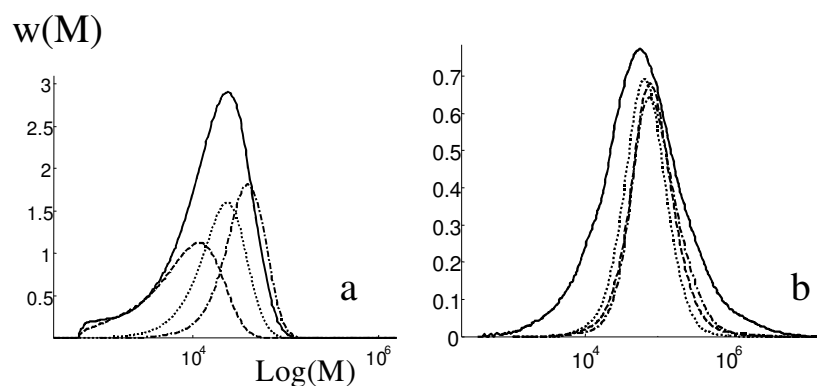


Figure 1: Molecular weight distributions. a) PC samples : PC1 (—), PC2 (---), PC3 (.....), PC4(- - - -), b) HDPE samples : PE1 (—), PE2 (---), PE3 (.....), PE4(- - - -)

**PS and HDPE:** Molar mass distributions are measured on a Waters Alliance GPC/V 2000 instrument with RI detection. Filtered samples are injected in the system at an injection volume of 150  $\mu\text{l}$  for PS and 323  $\mu\text{l}$  for HDPE. For PS samples, Styragel HR 6, 5, 4, 3 and 2 columns are used at a flow rate of 1 ml/min and, for HDPE samples, two Styragel HT6E and one Styragel HT2 columns are used at a flow rate of 1 ml/min for HDPE. Narrow PS standards covering the entire MW range of the samples are used for calibration purposes. For PS, the mobile phase is THF. Polymer concentration is 1 g/l and temperature 40°C. For PE, SEC is carried out at 135°C in 1,2,4-trichlorobenzene, stabilized with BHT (2 g/l). Polymer concentration is 2 g/l. The following Mark-Houwink relationships are used for universal calibration<sup>25,26</sup>:  $[\eta]_{\text{PS}} = 1.21 \cdot 10^{-4} * M^{0.71}$  (dl/g) and  $[\eta]_{\text{PE}} = 5.00 \cdot 10^{-4} * M^{0.706}$  (dl/g).

### 1.3.3 Rheological measurements

Dynamic storage and loss moduli,  $G'(\omega)$  and  $G''(\omega)$ , are determined with a strain-controlled rheometer (ARES from Rheometrics) in dynamic mode with a parallel-plate configuration at temperatures ranging from 140 to 200°C for PS, 160 to 220 °C for PC and 140 to 220°C for PE. Linearity of the viscoelastic regime is always checked beforehand with the help of a strain sweep. For PC, plates with a diameter of 8 mm are used, in order to conserve the small available quantities of fractionated samples. For PS and PE, the usual 25 mm diameter plates are used instead. The angular frequency sweep interval is  $10^{-2}$  to  $10^2$  rad/s, with a strain amplitude of 5 % for PS and HDPE. The corresponding values for PC are  $10^{-1}$  to  $5 \cdot 10^2$  for angular frequency and 15% for strain amplitude. All measurements are performed under dry nitrogen atmosphere.

Master curves (reference temperature of 170°C for PS, 200°C for PC and 190°C for PE) have been successfully calculated by applying the time-temperature superposition principle<sup>19,27</sup> with the help of the instrument software.

Table 6: Material, Rouse and TDD-DCDR model parameters for PS, PC and PE

Polymers	Me (g/mol)	$G_N^0$ (Pa)	$\beta$	K (s.(mol/g) <sup>3</sup> )	M* (g/mol)	$K_{\text{Rouse}}$ (s.(mol/g) <sup>2</sup> )
PS	18500	$2 \cdot 10^5$	2.25	$1.05 \cdot 10^{-15}$	160000	$2 \cdot 10^{-12}$
PC	2500	$1.2 \cdot 10^6$	2.25	$3.2 \cdot 10^{-14}$	50000	$2 \cdot 10^{-12}$
PE	1500	$2.6 \cdot 10^6$	2.25	$1.4 \cdot 10^{-17}$	70000	n.d.

Use of the theoretical models of Section II requires input data for  $M_e$  and  $G_N^0$  (Table 6). Literature data for PS<sup>9,11,15,19,28</sup> and PE<sup>15,19,28,29</sup> are relatively consistent. In the present work, we have used those given by Leonardi et al.<sup>3</sup>. The case of PC is quite different. The scatter of published<sup>28,30,31,32</sup> data for  $G_N^0$  and  $M_e$  is much larger than for PS and PE. The particular values selected here (Table 6) are very close to those of Jordan and Richards<sup>30</sup>.

### 1.3.4 Numerical implementation

The theoretical models described in Section II have been implemented in MatLab in order to predict the relaxation function  $G(t)$ . The function  $G(t)$  is in turn inverted to obtain dynamic moduli  $G'$  and  $G''$  by use of the well known Schwarzl relations<sup>33</sup>. This approximated method has been preferred over the Fourier Transform approach for its simplicity and associated computational speed (which becomes relevant for the inverse problem<sup>18</sup>). It provides excellent results in the frequency range of the experimental data, except perhaps at the lowest frequencies because of the well known series truncation issue<sup>33</sup>. In all cases (including monodisperse samples), full molecular weight distributions in discretized form are used to describe chain lengths rather than average values. Usually, distributions are discretized in 25 slices per decade. For each kind of polymer, optimization of material parameters is performed by minimizing the discrepancy between model predictions and experimental data for one (or two) selected

sample. Then, these values are used to predict the rheological curves of the others samples. The des Cloizeaux Time-dependent diffusion relaxation function has been implemented in the simplified form suggested by des Cloizeaux<sup>16</sup> and presented in Table 1.

## 1.4 RESULTS AND DISCUSSION

### 1.4.1 Comparison between reptation models for well entangled chains

We have first assessed the three major relaxation functions ( $F_{DE}$ ,  $F_{Fluct}$  and  $F_{TDD}$ ) outlined in Section II by comparing experimental dynamic moduli with model predictions for *well entangled* PS samples. Only results obtained for four samples (PS1, PS9, PS12 and PS13, see Table 3) are reported in detail here in Figures 2 to 4. They are indeed representative of all other observations.

In all cases, the model-dependent material parameters (defined in Table 1) have been fitted on PS9 and the optimal values have been used as such on all other samples and blends. We find the results independent of the particular sample chosen for the fit.

In principle, the double reptation exponent  $\beta$  should be equal to 2. However, for all the tested relaxation functions, we have found better agreement by *consistently* taking  $\beta$  equal to 2.25. This value slightly higher than 2 can be rationalized by the existence of some entanglements involving more than two chains. This value is also in agreement with the early tube dilation model proposed by Marrucci<sup>12</sup> and with recent results presented by Thimm et al.<sup>14</sup>.

The Rouse relaxation has been included in all cases in order to optimize the fit at high frequencies. This relaxation process does not depend on the choice of the relaxation function and therefore does not affect conclusions drawn for the reptation models. It is described by the single proportionality constant  $K_{Rouse}$ , which relates  $\tau_{Rouse}$  and  $M^2$ .

As expected, results obtained with the Doi and Edwards function  $F_{DE}$  (eq 1) are not satisfactory, because fluctuations effects are not taken into account (see Figure 2). In this case, the values of parameters  $K$  and  $\alpha$  are respectively  $2.5 \cdot 10^{-18}$  (s.(mol/g)<sup>3.4</sup>) and 3.4.

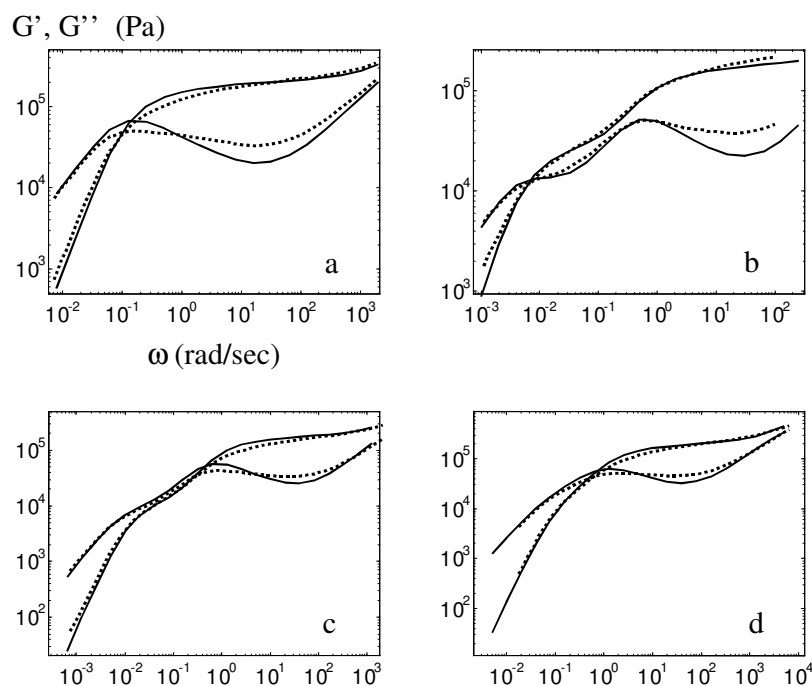


Figure 2: Experimental (...) and predicted (—) dynamic moduli for PS samples, with the Doi and Edwards kernel and double reptation for a) PS1, b) PS9, c) PS12, d) PS13.

By including fluctuation effects in the Doi and Edwards relaxation function (eq 2), we obtain a much better agreement between experimental and predicted data (see Figure 3). The fitted values for  $K$  and  $\nu$  are  $2.5 \cdot 10^{-15}$  (s.(mol/g)<sup>3</sup>) and 0.75.

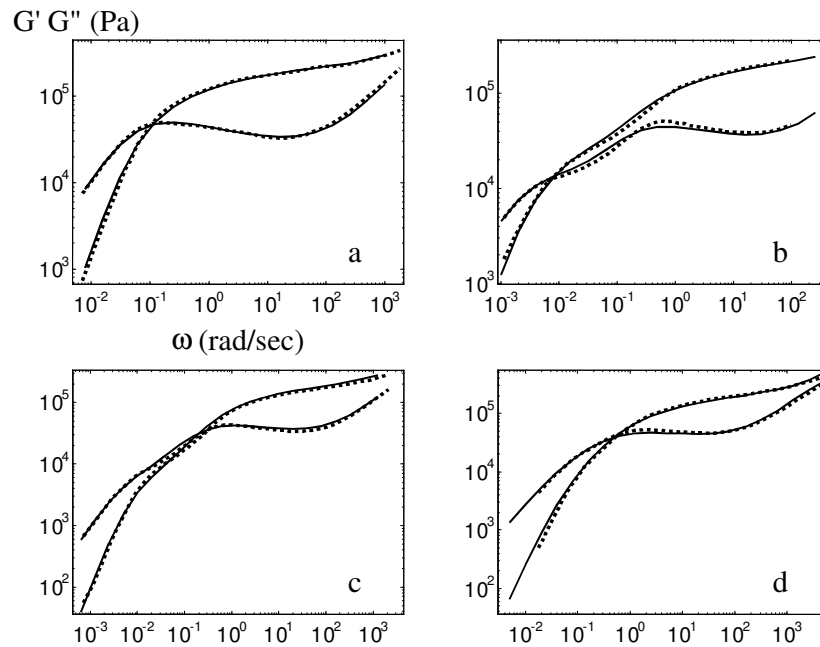


Figure 3: Experimental (...) and predicted (—) dynamic moduli for PS samples, with the Doi and Edwards kernel with fluctuations and double reptation for a) PS1, b) PS9, c) PS12, d) PS13.

The best results are systematically obtained with the Time-Dependent Diffusion des Cloizeaux function (eq 4) associated with double reptation model (eq 1 and 5). The fitted model parameters used in this case are reported in Table 6. The results are quantitatively correct within experimental error and give an even better fit than the fluctuations relaxation function as can be observed from Figure 4.

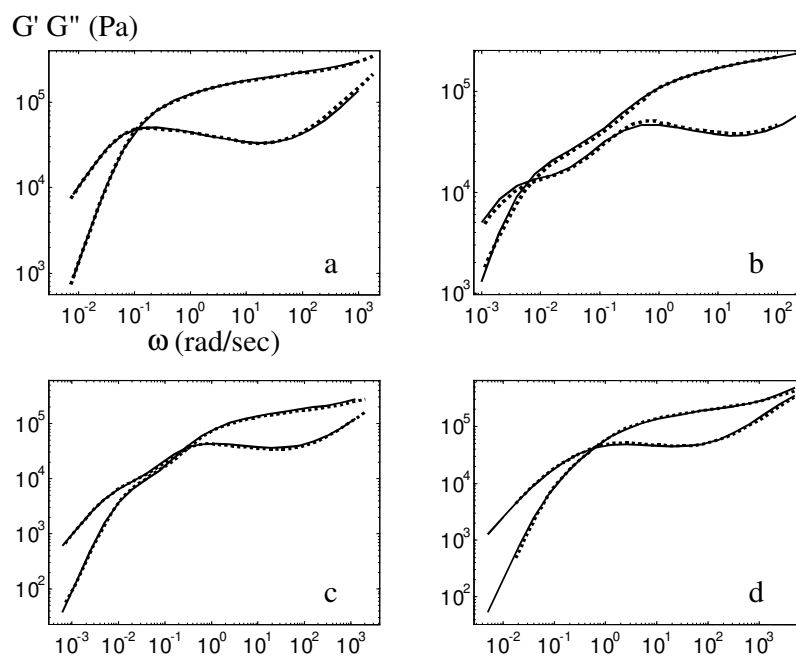


Figure 4: Experimental (...) and predicted (—) dynamic moduli for PS samples, with the des Cloizeaux kernel with fluctuations and double reptation for a) PS1, b) PS9, c) PS12, d) PS13.

From the above observations, we can conclude that it is essential to include fluctuation effects in the relaxation function even for highly entangled polymers, which could seem at first counterintuitive. The best results are obtained with the des Cloizeaux function which has also the advantage of providing a clearer picture of the physics involved and is eminently tractable in its “simplified” form. Therefore, we restrict ourselves for the remainder of this paper to analysis of the combination Time-Dependent Diffusion relaxation function - double reptation (TDD-DR). As will be shown in following sections, this combination also gives excellent results for PC and HDPE.

### 1.4.2 Relaxation of short chains with TDD-DR

Despite the excellent results obtained for highly entangled chains, the TDD-DR model is unable to correctly predict relaxation of short chains, i.e. with a molar mass less than about 4  $Me$ . This problem is visualized on Figure 5a for a PS blend comprising short chains (PS10, see Table 3), and on Figure 5b for the lowest molar mass PC fraction (PC2, see Table 4). Model predictions are clearly off the experimental data.

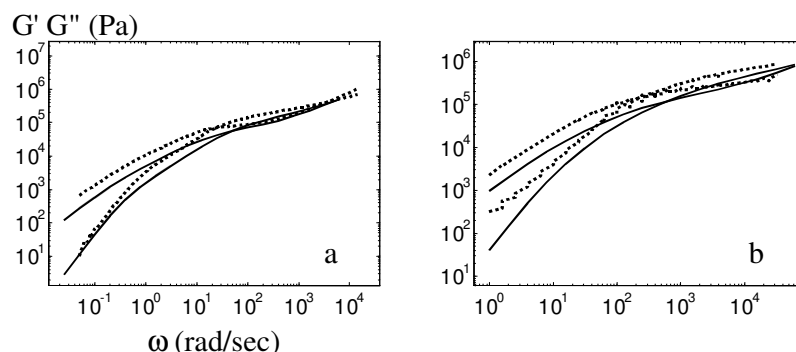


Figure 5: Experimental (...) and predicted (—) dynamic moduli for short chains sample a) PS10 and b) PC2, with des Cloizeaux kernel and des Cloizeaux double reptation.

Short chains are predicted to relax *too quickly* in comparison with experiments.

This problem finds its origin in the interaction between Rouse relaxation and reptation. For short chains, the reptation process begins before the end of the Rouse relaxation. This is shown in Figure 6 which compares Rouse relaxation and reptation as a function of time for a PS chain of mass 3  $Me$ . Both predictions by  $F_{DE}$  and  $F_{TDD}$  relaxation functions are presented. There is no time scale separation between the two processes as would be the case for longer chains. For instance, the des Cloizeaux function predicts 30% relaxation for the test chain after  $6 \cdot 10^{-4}$  seconds which is also the time needed by a tube

segment to relax by the Rouse process. Thus, 30% of this chain is predicted to relax by reptation before the end of the Rouse relaxation. The corresponding value for the Doi and Edwards function is only 5% relaxation by reptation at the same time.

The unavoidable conclusion is that the basic hypothesis that reptation and Rouse phenomena can be treated separately fails for “short” chains. This has already been observed by des Cloizeaux<sup>17</sup>.

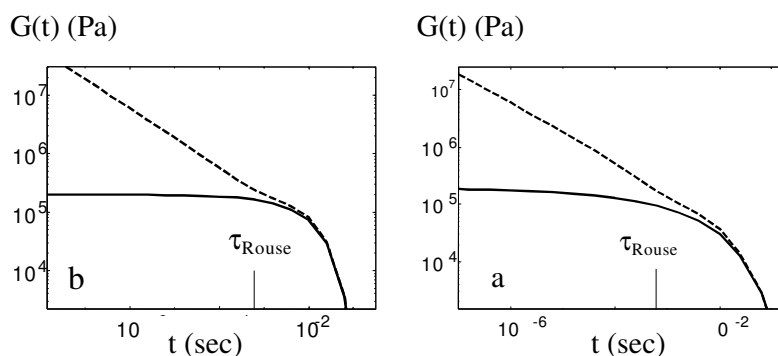


Figure 6:  $G(t)$  for a monodisperse polymer with a molar weight of 60000 g/mol. a) Doi and Edwards kernel, b) Des Cloizeaux kernel

Since our ultimate goal is practical, in particular by reference to the inverse problem, we have tried to empirically modify the TDD-DR model in order to slow down relaxation of short chains. We have tested several options, and the best results are obtained with a straightforward correction for short chains ( $M < 4Me$ ). For long chains ( $M > 4Me$ ), the relaxation modulus  $G(t)$  is given by equations 1, 4 and 5, and for short chains ( $M < 4Me$ ),  $F_{mono}$  becomes equal to  $F_{sr}$  in equation 5. The reptation time  $\tau_{rept}$  is rescaled to  $\tau_{rept} / \beta$  below  $4Me$  to ensure continuity of the reptation time on both sides of the model crossover.

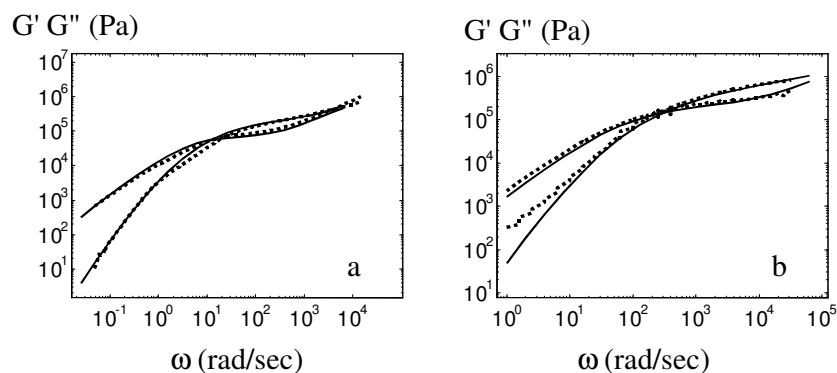


Figure 7: Experimental (...) and predicted (—) dynamic moduli for short chains PS10 and PC2 samples, by using the modified Time Dependent Diffusion – des Cloizeaux Double Reptation.

The results obtained with the modified TDD-DR model are shown in Figure 7 for the same samples as in Figure 5. The improvement is very significant and the prediction can now be considered quantitative.

The correction is admittedly empirical and the switch molar mass somewhat arbitrary, but it gives excellent results for all the polymers we have studied. Probably, it can further be improved by smoothing the transition over a molar mass range. The good quality of the correction may hint to some deeply rooted physical mechanisms although their exact nature is not clear.

### 1.4.3 Prediction of Viscosity and recoverable Compliance

Finally, before considering the other samples, it is useful to assess the predictions of the modified TDD-DR model for the zero-shear viscosity and recoverable compliance. These have been computed using the classical relations<sup>11</sup>:

$$\eta_0 = \lim_{\omega \rightarrow 0} \frac{G''(\omega)}{\omega} \quad (6)$$

$$J_e^0 = \lim_{\omega \rightarrow 0} \frac{G'(\omega)}{[G'(\omega)]^2 + [G''(\omega)]^2} \quad (7)$$

The results for the PS samples are given in Table 7, together with the corresponding experimental data as well as the predictions of the DE and tube fluctuation models. We also list in Table 7 the asymptotic frequency value at which the above relations are evaluated. We find that the predictions are in good agreement with the experimental data for all models. Overall, the modified TDD model is superior. It should be noted, however, that viscosity and compliance predictions only use information in the low-frequency range, where all models behave very similarly (cf Figures 2-4).

Table 7: Experimental and theoretical viscosity and Recoverable Compliance for the PS samples.

sample	$\omega$ ( $10^{-3}$ rad/sec)	$\eta_{0,\text{exp}}$ ( $10^4$ Pa s)	$\eta_{0,\text{theor.}}$ ( $10^4$ Pa s)	$J_{e,0}^{\text{exp}}$ ( $10^{-5}$ Pa $^{-1}$ )	$J_{e,0}^{\text{theor.}}$ ( $10^{-5}$ Pa $^{-1}$ )	model
PS1	6	104	105	1.3	1.26	TDD
PS1	6	104	95	1.3	0.79	DE
PS1	6	104	107	1.3	1.44	FLUC
PS9	1.12	435	490	6.65	4.84	TDD
PS9	1.12	435	433	6.65	4.06	DE
PS9	1.12	435	443	6.65	5.51	FLUC
PS10	1.12	1.33	1.33	3.32	3.25	TDD
PS10	1.12	1.33	1.07	3.32	2.52	DE
PS10	1.12	1.33	1.50	3.32	6.43	FLUC
PS12	1.14	94.2	97.7	9.38	9.34	TDD
PS12	1.14	94.2	89.3	9.38	7.79	DE
PS12	1.14	94.2	95.8	9.38	11	FLUC
PS13	1.78	24.6	25	2.5	3.01	TDD
PS13	1.78	24.6	25.9	2.5	1.93	DE
PS13	1.78	24.6	26.5	2.5	3.19	FLUC

#### 1.4.4. Polycarbonate samples: overall comparison between theory and experiments

Figure 8 compares predictions by the modified TDD-DR model and experimental dynamic moduli for the remaining PC samples (see Table 4). Results are shown for a commercial sample with relatively broad molar mass distribution (PC1), and for fractions with high and a medium molar mass (PC3 & PC4). Although the molar mass between entanglements of PC (2500 g/mol) is very small in comparison with the one for PS (18500 g/mol), and the samples cover a wide range of molar masses (by PC standards), quantitatively correct results are obtained for all samples.

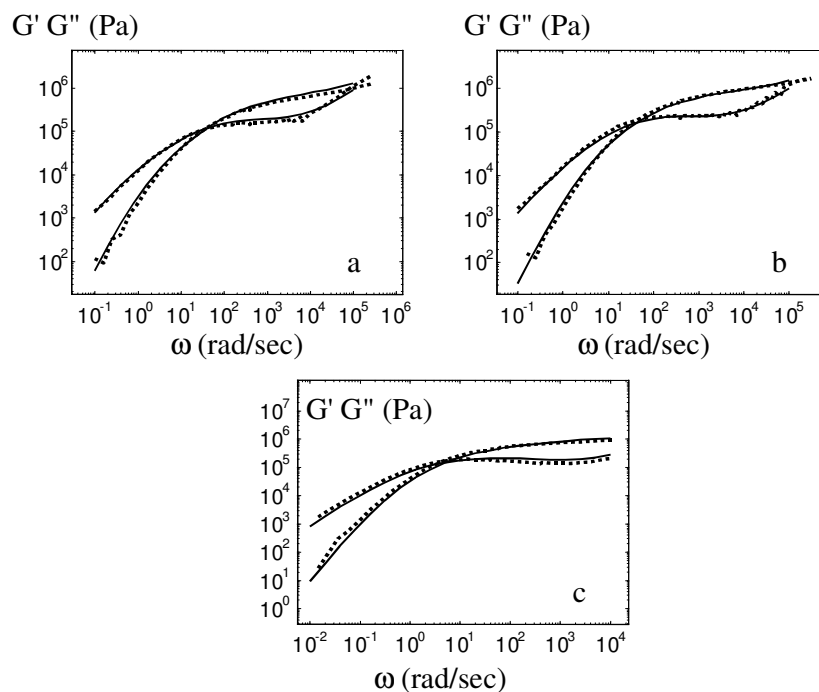


Figure 8: Experimental (...) and predicted (—) dynamic moduli for PC samples. A) PC1, b) PC3, c) PC4, with the modified TDD-DCDR model.

### 1.4.5 High density polyethylene

In order to further extend our test of the TDD-DR model, we have analyzed several HDPE samples (see Table 5). Comparison between predicted dynamic moduli and experimental data is presented in Figure 9 for a sample with a broad molar mass distribution (PE1) as well as three relatively narrow fractions (PE2, 3 and 4). Again, the model is able to reproduce  $G'$  and  $G''$  data very accurately. It is true that the test is less critical for PE than it is for PS or PC because of the narrower dynamic range experimentally accessible. However, it is a nice extension to a flexible chain polymer having a low  $Me$  value.

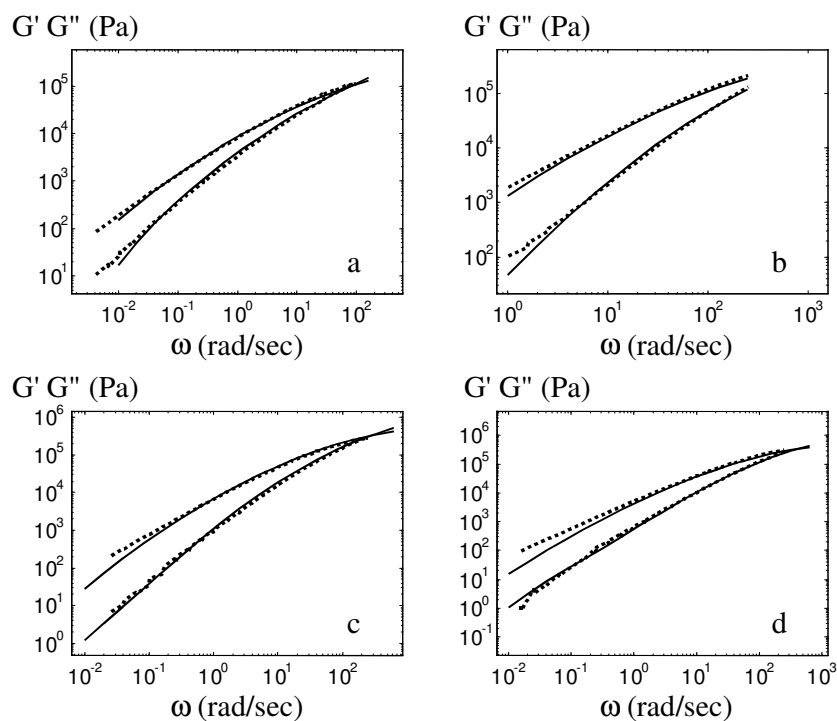


Figure 9: Experimental (...) and predicted (—) dynamic moduli for HDPE samples. a)PE1, b)PE2, c)PE3, d)PE4.

## 1.5 CONCLUSIONS

From analysis of almost monodisperse, bidisperse or polydisperse PS samples with high degree of entanglement, we conclude that the time-dependent diffusion des Cloizeaux relaxation function performs better than the fluctuations relaxation function when combined with double reptation. A mixing rule exponent  $\beta$  around 2.25 provides a better fit than the original value of 2. This could point toward the importance of multiple entanglements and is consistent with recently published data<sup>8,9,12</sup>. We also observe that it is essential to take tube length fluctuations into account even for highly entangled polymers. The combination of TDD with double reptation provides truly quantitative predictions for high  $MW$  PS blends. However, when this model is extended to systems containing a significant fraction of short chains ( $M < 4M_e$ ), it predicts too fast a relaxation. This problem is clearly linked to an overlap between the Rouse and reptation dynamics for short chains. While there is no complete answer to the issue, we suggest a simple modification of TDD-DR which gives quantitative prediction even for the shortest chains. The proposed relaxation function crossover for chains with  $M < 4M_e$  is empirical but may point to deep rooted physics. The modified TDD-DR model not only works for a very broad range of PS molar masses but also for broad ranges of PC and HDPE molar masses, and hence seems to enjoy a very wide range of validity. Our results confirm that there is no universal relationship between the TDD parameter  $M^*$  and  $M_e$  (see Tables 6). The best-fit ratio  $M^*/M_e$  is found to increase with decreasing  $M_e$ , from 8.7 for PS ( $M_e=18500$ ), to 20 for PC ( $M_e=2500$ ), and 47 for PE ( $M_e=1500$ ). It is important to notice that the quality of the fit is not very sensitive to the exact value of  $M^*$ .

Finally, the crossover from the reptation-dominated to the Rouse-dominated region is correctly described by the modified Rouse dynamics used in this paper.

In the companion paper<sup>18</sup>, we will apply the modified TDD-DR model and Rouse model for solving the inverse problem, using the same experimental systems.

**REFERENCES**

- [1] de Gennes, P.-G. *J. Chem. Phys.* **1971**, *55*, 572
- [2] Doi, M. ; Edwards, S. F. *The Theory of Polymer Dynamics*; Clarendon Press, **1986**; Chapter 6
- [3] Léonardi, F.; Majesté, J. C. ; Allal, A. ; Marin, G. *J. Rheol.* **2000**, *44*, 675
- [4] Pattamaprom, C.; Larson, R. G.; Van Dyke, T. J. *Rheol. Acta* **2000**, *39*, 517
- [5] Tsenoglou, C. *ACS Polym. Preprints* **1987**, *28*, 185
- [6] des Cloizeaux, J. *Europhys. Lett.* **1988**, *5*, 437
- [7] Graessley, W. W. *Adv. Pol. Science* **1982**, 47
- [8] Rubinstein, M.; Helfand, E.; Pearson, D. S. *Macromolecules* **1987**, *20*, 822
- [9] Maier, D.; Eckstein, A.; Friedrich, C; Honerkamp, J. *J. Rheol.* **1998**, *42*, 1153
- [10] Tsenoglou, C. *Macromolecules* **1991**, *24*, 1762
- [11] Wasserman, S. H.; Graessley, W. W. *J. Rheol.* **1992**, *36*, 543
- [12] Marrucci, G. *J. Polym. Sci.* **1985**, *23*, 159
- [13] Mead, D. W. *J. Rheol.* **1994**, *38*, 1797
- [14] Thimm, W.; Friedrich, C; Maier, D.; Marth, M.; Honerkamp, J. *J. Rheol.* **2000**, *44*, 429
- [15] Carrot, C; Guillet, J. *J. Rheol.* **1997**, *41*, 1203
- [16] des Cloizeaux, J. *Macromolecules* **1990**, *23*, 4678
- [17] des Cloizeaux, J. *Macromolecules* **1992**, *25*, 835
- [18] van Ruymbeke, E; Keunings, R.; Bailly, C.; “*Linear Viscoelasticity of Polydisperse Linear Polymers : Determination of the MWD from Rheological data, J.N.N.F.M*”
- [19] Ferry, J. D. *Viscoelastic Properties of Polymers*; Wiley, New York, **1980**
- [20] Aklonis, J. J.; MacKnight, W. J.; *Introduction to Polymer Viscoelasticity*, Wiley (New York), **1982**
- [21] Weinmann, K.; Wolf, B. A.; Rätzsch, M. T.; Tschersich, L. *J. Appl. Polym. Sci.* **1992**, *45*, 1265
- [22] Hagenars, A.; Pesce, J.-J.; Bailly, Ch.; Wolf, B.A. *Polymer* **2001**, *42*, 7653

- [23] Stéphenne, V; Bailly, C; Berghmans, H; Daoust, D; Godard, P; *Successive Solution Fractionation (SSF: a method to produce narrow dispersed Polyethylenes)*, in preparation
- [24] Berry, G.C.; Nomura, H.; Mayhan, K.G. *J. Polym. Sci.* **1967**, A2-5, 1-21
- [25] Otocka, E.P.; Roe, R.J.; Helamn, N.Y.; Muglia, P.M. *Macromolecules* **1971**, 4, 507
- [26] Scheinert, W. A. *Makromol. Chem.* **1977**, 63, 117
- [27] Macosko, C; *Rheology: Principles, Measurements and Applications*; Wiley-VCH, **1994**
- [28] Fetters, L. J.; Lohse, D. J.; Richter, D.; Witten, T. A.; Zirkel, A. *Macromolecules* **1994**, 27, 4639
- [29] Aharoni, S. M. *Macromolecules* **1986**, 19, 426
- [30] Jordan, T. C.; Richards, W. D.; in: Legrand, D. G.; Bendler J. T. (Eds.) *Handbook of Polycarbonate Science and Technology*; M. Dekker, New York, **2000**, chap. 9
- [31] Wimberger-Friedl, R.; Hut, M. G. T.; Schoo, H. F. M. *Macromolecules* **1996**, 29, 5453
- [32] Wu, S. *Poly. Eng. Sci.* **1992**, 32, 823
- [33] Schwarzl, F. R. *Rheol. Acta* **1971**, 10, 166

## APPENDIX II.2

### DETERMINATION OF MWD FROM G' AND G''

*E. van Ruymbeke, R. Keunings, C. Bailly*

#### 2.1 INTRODUCTION

Over the last two decades, a number of publications (most notably [2-11]) has been devoted to the prediction of the molecular weight distribution,  $\alpha(M)$ , of entangled linear polymers from their linear viscoelastic response. Although a considerable degree of success has been reached in the recent studies, more quantitative and robust predictions are yet to be obtained, specially for multimodal distributions. The variety of published models and techniques can be briefly described as follows.

First, on the theoretical side, two basic ingredients are used: (i) an analytical expression for the relaxation modulus,  $G_{mono}(t, M)$ , of the monodisperse system as a function of molecular weight,  $M$ , and (ii) a suitable mixing rule which relates the relaxation modulus of the polydisperse material,  $G(t)$ , to  $\alpha(M)$  and  $G_{mono}(t, M)$ . Ideally, the resulting mathematical model should have but few material parameters endowed with a clear physical or molecular interpretation. Over the years, various refinements of the classical de Gennes/Doi/Edwards reptation theory [12-13] have been used to model  $G_{mono}(t, M)$ , while mixing rules based on the Tsenglou/des Cloizeaux concept of Double reptation [14-16] have gained acceptance.

Results reported recently in [19] and the companion paper [1] show that quantitative predictions are indeed obtained with such molecular models in the *direct* problem (from MWD to linear viscoelastic properties) of computing